Title: Development of a field-deployable method for simultaneous, real-time measurements of the four most abundant N_2O isotopocules

Erkan Ibraim[a,b], Eliza Harris[a, 1], Simon Eyer[a], Béla Tuzson[a], Lukas Emmenegger[a], Johan Six[b] and Joachim Mohn[a]

[a]*Empa, Swiss Federal Laboratories for Materials Science and Technology, Laboratory for Air Pollution / Environmental Technology, CH-8600 Dübendorf, Switzerland*

[b]*ETH-Zürich, Swiss Federal Institute of Technology, Department of Environmental Systems Science, CH-8092 Zürich, Switzerland*

(Received xx January 2017; final version received xxx)

Corresponding author: E-mail: erkan.ibraim@empa.ch; Phone: + 41 58 765 49 01

Eliza Harris: E-mail: eliza.harris@uibk.ac.at; Phone: + 43 670 206 7687

Simon Eyer: E-mail: simon.eyer@gmail.com; Phone: + 41 788234522

Béla Tuzson: E-mail: bela.tuzson@empa.ch; Phone: + 41 58 765 46 42

Lukas Emmenegger: E-mail: lukas.emmenegger@empa.ch; Phone: + 41 58 765 46 99

Johan Six: E-mail: jsix@ethz.ch; Phone: +41 44 632 84 83

Joachim Mohn: E-mail: joachim.mohn@empa.ch; Phone: + 41 58 765 46 87

This work was supported by the Swiss National Science Foundation under Grant No. 200021L_150237.

[1] *New Affiliation: University of Innsbruck, Institute of Ecology, A-6020 Innsbruck, Austria*

Abstract: Development of a field-deployable method for simultaneous, real-time measurement of the four most abundant N_2O isotopocules

Understanding and quantifying the biogeochemical cycle of N_2O is essential to develop effective N_2O emission mitigation strategies. This study presents a novel, fully-automated measurement technique that allows simultaneous, high-precision quantification of the four main N_2O isotopocules ($^{14}N^{14}N^{16}N$, $^{14}N^{15}N^{16}O$, $^{15}N^{14}N^{16}O$ and $^{14}N^{14}N^{18}O$) in ambient air. The instrumentation consists of a trace gas extractor (TREX) coupled to a quantum cascade laser absorption spectrometer (QCLAS), designed for autonomous operation at remote measurement sites. The main advantages this system has over its predecessors are a compact spectrometer design with improved temperature control and a more compact and powerful TREX device. The adopted TREX device enhances the flexibility of the TREX technique for higher adsorption volumes to target rare isotopic species and lower adsorption temperatures for highly volatile substances. All system components have been integrated into a standardized instrument rack to improve portability and accessibility for maintenance. With an average sampling frequency of approximately 1 hr^{-1}, this instrumentation achieves a repeatability of 0.09, 0.13, 0.17 and 0.12 ‰ for $\delta^{15}N^{\alpha}$, $\delta^{15}N^{\beta}$, $\delta^{18}O$ and site preference of N_2O, respectively, for pressurized ambient air. The repeatability for N_2O mole fraction measurements is better than 1 ppb (parts per billion, 10^{-9} moles per mole of dry air).

Keywords: nitrous oxide isotopic composition; atmospheric measurement techniques; trace gas analysis, preconcentration, quantum cascade laser spectrometer.

1 Introduction

The atmospheric abundance of the dominant stratospheric ozone depleting substance and strong greenhouse gas (GHG) [1, 2] nitrous oxide (N_2O) has increased from 270 ppm in pre-industrial times to 328.0 ± 0.1 ppb in 2015 [3, 4]. In order to achieve emission reduction targets a detailed understanding of the temporal and spatial variations in N_2O emissions is required [5, 6, 7]. Atmospheric N_2O isotopic composition provides important information about N_2O source processes because distinct microbial and abiotic pathways exhibit characteristic

isotopic signatures [8, 9]. Apart from the main N_2O isotopic species, $^{14}N^{14}N^{16}N$, contributing 99 % of total atmospheric N_2O, the three most abundant isotopocules (constitutional isotopomers) are $^{14}N^{15}N^{16}O$ (^{15}N at position α), $^{15}N^{14}N^{16}O$ (^{15}N at position β) and $^{14}N^{14}N^{18}O$ [10, 11]. Abundances of isotopocules are usually reported in the δ-notation in per mil (‰), $\delta^{15}N^{\alpha}$, $\delta^{15}N^{\beta}$, $\delta^{18}O$, which indicates the relative difference of the isotopic ratios of the less and most abundant isotopic species between the sample and the standard [12]. The international isotope ratio scale for ^{15}N / ^{14}N is atmospheric N_2 (AIR-N2) and for ^{18}O / ^{16}O Vienna Standard Mean Ocean Water (VSMOW). The thermal decomposition of isotopically characterized ammonium nitrate (NH_4NO_3) has been suggested as an approach to link the position-dependent nitrogen isotopic composition of N_2O to AIR-N2 [10, 13]. The ^{15}N content of a sample gas is usually reported as the bulk ^{15}N content ($\delta^{15}N^{bulk} = [\delta^{15}N^{\alpha} + \delta^{15}N^{\beta}] / 2$), while the site preference (SP) is used to denote the intramolecular ^{15}N distribution ($SP = \delta^{15}N^{\alpha} - \delta^{15}N^{\beta}$) [14, 15].

The standard technique for analysis of N_2O isotopic composition is isotope-ratio mass-spectrometry (IRMS) [10], which is capable for high-precision and high-sensitivity measurement [16]. However, IRMS instruments are bulky and not designed for field deployments. Recently, quantum cascade laser absorption spectroscopy (QCLAS) [17] and cavity ring-down spectroscopy (CRDS) [18] were introduced as alternative techniques for N_2O stable isotope analysis, capable of measuring in real time even at remote locations [19, 20, 21]. A further advantage of laser spectroscopy is its ability for direct selective analysis of intramolecular isotopic isomers (isotopomers) such as $^{14}N^{15}N^{16}O$ and $^{15}N^{14}N^{16}O$, which can only be determined indirectly by the analysis of NO^+ fragment ions using mass spectrometry. Several studies have successfully applied QCLAS and CRDS spectrometers for N_2O isotope analysis in laboratory and field-site incubation experiments [18, 22, 23], and more recently, to analyse diurnal and seasonal variations of ambient N_2O [24, 25]. Isotopic source signatures are determined from ambient measurements using the traditional two end-member mixing

models, i.e. “Keeling plot” approach [26], or the Miller – Tans plot if the stable background requirement is violated [27].

Although N_2O isotope analysis with combined preconcentration and subsequent dual QCLAS analysis has previously been published, the capability of this instrumentation in field applications was still limited. In this study, we implemented a more compact and powerful preconcentration device (TREX) and further developed the field-applicability of the TREX-QCLAS technique for high-precision in-situ measurements of the four most abundant N_2O isotopic species by utilizing a single QCLAS and enhancing its temperature stability. In addition, all system components were integrated into an instrument rack to improve portability and reduce maintenance effort. The developed analytical instrumentation can also be applied to other rare or highly volatile target substances, due to the enhanced performance of the preconcentration device regarding adsorption volume and temperature. This paper summarizes the technological approach and the improvements made during these developments. It represents the first detailed description of the TREX unit used here, which can be employed in combination with various laser spectrometers, and possibly other analytical technologies.

2 Materials and methods

The instrumentation in this study consists of a QCLAS coupled to a TREX device. A predecessor model with similar functionality but higher space requirements and limited application possibilities has been previously published [28, 29, 30]. The TREX-QCLAS instrumentation in this study is optimized to simultaneously measure the four most abundant N_2O isotopocules under field conditions, by significantly improving spectrometer temperature stability (as presented in section 3.1.2) and building the overall system into a 19” instrument rack. An overview of the TREX-QCLAS set up is provided in Figure 1, and in Figure 2, a detailed gas flow scheme is given.

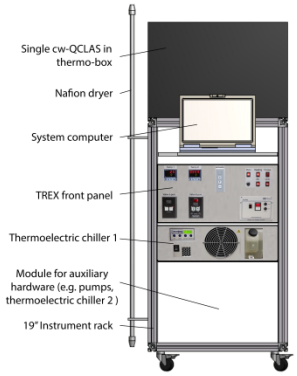

Figure 1 Technical drawing of the 19" instrument rack with major components: single cw-QCLAS, nafion dryer, tracegas extractor (TREX), and thermoelectric chiller. Outer dimensions of the instrumentations are 1.75 m × 0.95 m × 0.65 m (length × width × height).

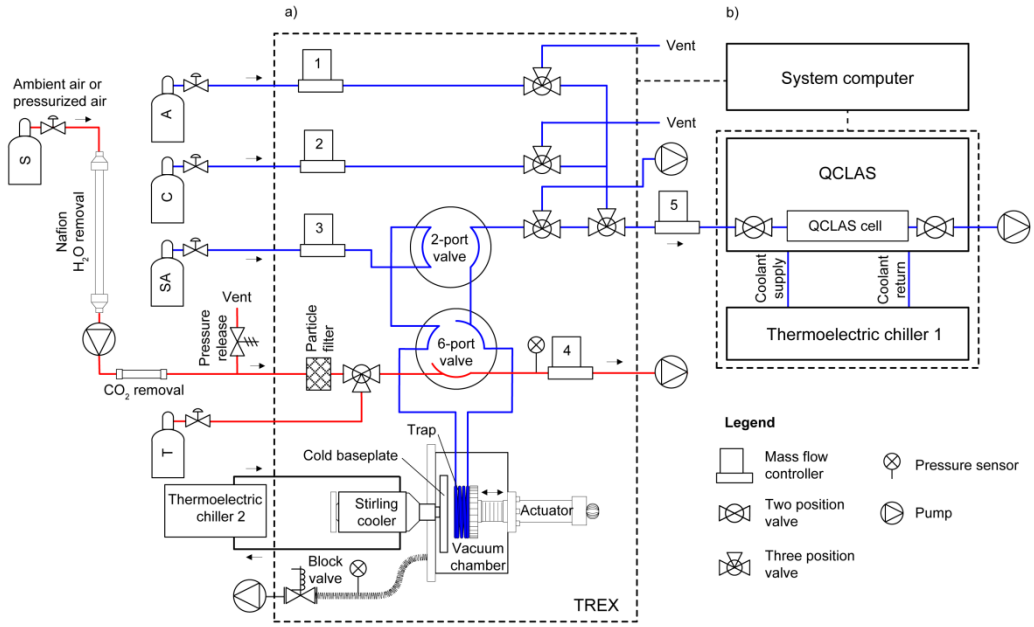

Figure 2 a) Flow scheme of the trace gas extractor (TREX) and b) the quantum cascade laser absorption spectrometer (QCLAS) as well as auxiliary devices, i.e. system computer, thermoelectric chiller. The illustrated setting represents phase V in Figure 4 (regeneration of the trap).

2.1 Preconcentration of ambient N_2O using TREX

Key elements to control the gas flow in the TREX device (Figure 2) are five mass flow controllers (MFCs) (Redy Smart series, Vögtlin Instruments, Switzerland), a four-port two-position and a six-port multi-position valve (Valco Instruments Inc., Switzerland), and a number of two- and three-position solenoid valves (Parker Hannifin Corp., USA). Prior to preconcentration, the sample gas is dehumidified using a permeation dryer (PermaPure Inc., USA). Downstream of the pump (PM 25032-022, KNF Schweiz AG, Switzerland), remaining humidity and CO_2 are removed using a trap filled with Ascarite (6 g, 10 - 35 mesh, Fluka, Swit-

zerland) bracketed with magnesium perchlorate ($Mg(ClO_4)_2$, 2 × 1.5 g, Fluka, Switzerland). For N_2O preconcentration, the sample gas is pumped through the adsorption trap (HayeSep D, Sigma Aldrich, Switzerland) at a flow rate of 500 mL min^{-1}. N_2O adsorption is terminated after 5.080 ± 0.011 L of sample gas have passed through the adsorption trap, which is kept at 125.1 ± 0.1 K during adsorption using a high power Stirling cryo-cooler (CryoTel GT, Sunpower Inc., USA) in combination with a compact thermoelectric chiller (Oasis, Solid State Cooling Systems Inc., USA). The adsorption trap temperature represents a trade-off between quantitative N_2O adsorption on the trap, and passage of bulk air constituents (e.g. N_2, O_2, Ar) as well as a number of more volatile trace gases (e.g. CO, CH_4), which would otherwise introduce spectral interferences. For N_2O desorption, the trap is decoupled from the cold copper baseplate using an actuator (ZLD225MM, VG Scienta Ltd, UK). Subsequently, the trap is heated stepwise to 175 K, using a heat foil (diameter 62.2 mm, 100 W, HK5549, Minco Products Inc., USA) controlled by a PID temperature controller (cTron, Jumo Mess- und Regeltechnik AG, Switzerland), while being purged with 1 - 5 mL min^{-1} synthetic air to remove co-adsorbed gases (e.g. O_2, CO). Thereafter, the trap is heated further to 275 K and the N_2O desorbed from the trap is purged into the spectrometer cell with 1 mL min^{-1} synthetic air. This procedure yields a N_2O mole fraction of 90 ± 0.3 ppm (parts per million, 10^{-6} moles per mole of dry air) in the QCLAS cell at a cell pressure of 20 ± 0.02 hPa (6.04 μmol), which is equivalent to a preconcentration factor of 272.

Relevant TREX-QCLAS parameters are controlled by a system computer via a 16-port serial-to-ethernet network connector (Etherlite 160, Digi International Inc., USA). A custom-written LabVIEW (National Instruments Corp., USA) software allows remote control and scheduled automatic operation of the TREX.

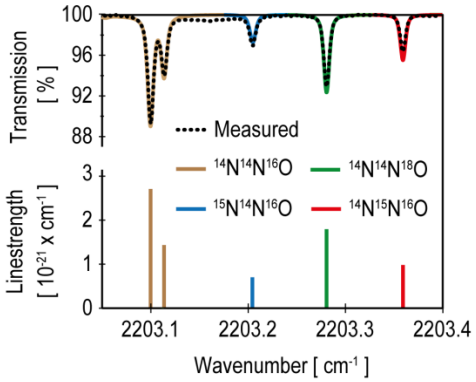

Figure 3 Transmission spectra (on the top) and linestrength (on the bottom) of $^{14}N^{14}N^{16}O$, $^{15}N^{14}N^{16}O$, $^{14}N^{14}N^{18}O$ and $^{14}N^{15}N^{16}O$, respectively. Solid lines refer to Hitran data [39], while the dashed line represents experimental data as obtained in this study. CO absorption occurs between the lines $^{14}N^{14}N^{16}O$ and $^{15}N^{14}N^{16}O$ (at 2203.16 cm^{-1}), if CO is present in the analyte gas (not shown in the Figure). To avoid spectral interferences, CO is largely removed during preconcentration.

2.2 Laser spectrometer

Laser-based trace gas analysers have been developed and used for more than 10 years [19, 31, 32]. A significant step for their field deployment and performance was the development of room temperature QCLs and many subsequent instrumental improvements [33, 34]. The focus of this study was to further enhance the field-applicability of QCLAS. To meet this target, we defined the appropriate spectral region and implemented a corresponding laser source to a commercially available compact instrument (CW-QC-TILDAS-76-CS; Aerodyne Research Inc., Billerica, USA). This spectrometer comprises a continuous-wave (cw) mid-infrared quantum cascade laser source emitting at 2203 cm^{-1} and an astigmatic multi-pass absorption cell with a path length of 76 m and a volume of approximately 0.62 L [35]. Laser control, data acquisition and quantification of the four most abundant N_2O isotopic species, $^{14}N^{14}N^{16}N$, $^{14}N^{15}N^{16}O$, $^{15}N^{14}N^{16}O$ and $^{14}N^{14}N^{18}O$ (Figure 3), are performed using TDL Wintel software (Aerodyne Research Inc., Billerica, USA).

2.3 Calibration gases and target gas

Table 1 provides detailed information on the isotopic composition and N_2O mole fractions of the two standard gases and the pressurized air target gas used in this study. The two standard gases, anchor (A) gas and calibration (C) gas, were applied for the drift correction and for the two-point calibration. Pressurised air target (T) gas was used to investigate the system per-

formance. A and C were produced by dynamic dilution of pure medical N_2O (Pangas, Switzerland) with isotopically pure (> 98 %) $^{14}N^{15}N^{16}O$ (Cambridge Isotope Laboratories, USA), pure (99.95 %) $^{14}N^{14}NO$ (ICON Services Inc., USA) and gravimetrically diluted with high-purity synthetic air (99.999 %, Messer Schweiz AG) to yield a final N_2O mole fraction of approximately 90 ppm. Gas A was tailored towards ambient isotopic composition and used as an anchor to link measurements to the international isotope ratio scales. C was produced with lower $\delta^{15}N^{\alpha}$, $\delta^{15}N^{\beta}$ and $\delta^{18}O$ values compared to A, and is used as the second point in a two-point calibration. To correct for the dependence of isotope ratios on N_2O mole fractions, A is additionally measured diluted to a mole fraction of 55 ppm. N_2O mole fractions of A, C and T were measured and compared to standards provided by commercial suppliers (A, C) and the National Oceanic and Atmospheric Administration/ Earth System Research Laboratory/ Global Monitoring Division (NOAA/ ESRL/ GMD) (T). The N_2O isotopic composition of A and C were linked to standard gases analysed by Sakae Toyoda at Tokyo Institute of Technology (TIT), while T was analysed against A and C at Empa and results were compared to IRMS measurements at TIT to determine the compatibility of the TREX-QCLAS technique.

Table 1 Overview of N_2O isotope delta values of the standard gases (A, C) and the target gas (T) as analysed at Empa against standards previously analysed by Sakae Toyoda/ Tokyo Institute of Technology. The standard gas A (anchor) is used for drift correction, and standard gas C for a span correction of measured δ values. The mole fraction of A and C is approx. 90 ppm, while the mole fraction of T is approx. 329 ppb. The precision indicated is the standard deviation for replicate sample measurements and does not include the uncertainties of the calibration chain.

Tank	$\delta^{15}N^{\alpha}$ [‰]	$\delta^{15}N^{\beta}$ [‰]	$\delta^{18}O$ [‰]
A	15.51 ± 0.30	-3.25 ± 0.20	34.97 ± 0.16
C	-63.08 ± 0.78	-59.81 ± 0.48	27.99 ± 0.28
T	15.25 ± 0.09	-3.37 ± 0.13	43.80 ± 0.17

2.4 Data evaluation

The data evaluation presented here follows the principles as presented by Eyer et al. [20] and Harris et al. [25] and is discussed in brief here. The mole fraction data for N_2O isotopocules obtained with TDL Wintel and the calculated isotope ratios are evaluated and calibrated to the international isotope ratio scales using Matlab (MathWorks, Inc., USA). As a first step, a drift

correction is applied to all data based on the drift observed in A, which accounts for any systematic error that may occur over time due to unintended system parameter changes (e.g. due to ambient temperature). A moving average of two anchor points is used to calculate the correction. In addition, a correction based on linear regression is performed to account for systematic errors caused by laser frequency drifts, cell pressure and temperature. Then, the drift correction is repeated for the intermediate results and, finally, a two-point calibration based on A and C isotopic composition is applied to all data, yielding final δ values referenced to international isotope ratio scales.

N_2O mole fractions in the sample gas before preconcentration are determined by applying an one-point calibration to the measured N_2O mole fractions and accounting for the preconcentration factor calculated from the following factors (errors refer to one sigma standard deviation among repeated measurements): absorption cell volume (0.62 L), cell pressure (20 ± 0.02 hPa) and trapped sample volume (5.080 ± 0.011 L).

3 Results and discussion

3.1 Optimization of preconcentration and spectrometer

3.1.1 Preconcentration of ambient N_2O using TREX

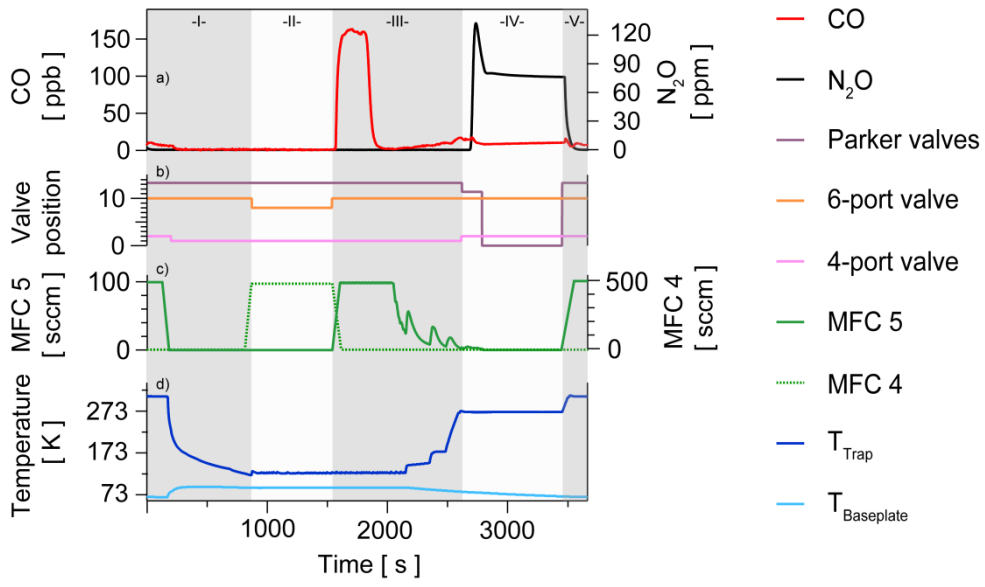

Figure 4 Typical sequence of a full preconcentration cycle: In phase I, the trap is attached to the Stirling-cooled baseplate to cool it down to the target temperature (125 K). Once the target temperature is reached, phase II is initiated by switching the six-port multi position valve to the appropriate position (orange line). Thereby sample gas at a flowrate of 500 mL min^{-1} is directed towards the trap. After adsorbing 5 L of sample gas phase II is ceased, and in

phase III, the trap is purged with synthetic air to remove co-adsorbed, bulk air constituents (e.g. O_2) or trace gases (e.g. CO) from the trap. Finally, in phase IV, N_2O is desorbed and purged into the QCLAS cell for analysis. During phase V, the trap is conditioned, i.e. reset to initial conditions, by heating it to 308 K and purging with synthetic air.

Figure 4 schematically shows the sequence of a full preconcentration procedure as developed within this study. The procedure consists of five phases: In phase I, the adsorbent trap is coupled to the Stirling-cooled baseplate (around 63 K) and cooled to the target temperature (125 K). Once the target temperature is reached, phase II begins, in which N_2O is preconcentrated from ambient air by passing sample gas through the adsorption trap at 500 mL min^{-1}. Phase II is initiated by switching the 6-port multi-position valve, thereby directing the sample gas flow through the trap. This phase is ceased once 5.080 ± 0.011 L of ambient air have passed through the trap by resetting the multi-position valve as shown in Figure 4. During phase III, residual bulk air components (e.g. O_2, N_2) and co-adsorbed spectrally interfering trace gases (e.g. CO, CH_4) are removed from the adsorption trap, which is a preparatory step before N_2O desorption. Phase III starts with switching the multi-position valve and thereby enabling 100 mL min^{-1} synthetic air to flow through the trap and thereby purge out co-adsorbed substances (e.g. CO, red curve in Figure 4). This step was found to be essential for accurate measurements, since absorption bands of some gases would otherwise overlap and interfere with existing N_2O bands. Furthermore, by increasing the trap temperature stepwise any residual bulk gases (e.g. O_2, N_2) are desorbed, which is a prerequisite to achieve a defined and repeatable gas matrix (solid green line Figure 4). Changes in the gas matrix were previously shown to affect N_2O and CH_4 isotope analysis [18, 20] but not specifically tested within this study. In phase IV, N_2O is desorbed from the trap into the QCLAS cell by switching the four-port two-position valve and thereby directing the synthetic air flow through the trap into backward direction and increasing the trap temperature to 278 (Figure 4). Desorption is ceased when the pressure in the gas cell reaches 20 hPa. Finally, the trap is regenerated by being heated to 308 K while being purged with 100 mL min^{-1} synthetic air for five minutes (phase V).

Quantitative N_2O recovery, i.e. the absence of N_2O breakthrough as well as complete N_2O desorption, was tested and ensured with a number of specifically tailored experiments. To test the completeness of adsorption, N_2O from pressurized ambient air at 329 ppb N_2O was adsorbed on the trap, but phase II (adsorption) was extended and N_2O mole fractions were analysed at the outlet of MFC 4 (see Figure 2) using a single cw-QCLAS (2199.7 cm^{-1}, CW-QC-TILDAS-76-CS; Aerodyne Research Inc., Billerica, USA) with a detection limit of 0.05 ppb N_2O [36]. The determined breakthrough volume of > 500 L, well above the volume needed in this study (around 5 L), underlines the potential of the TREX device for the preconcentration of large amounts of air for measurement of rare N_2O isotopic species (e.g. doubly substituted isotopes) or other very rare trace gases. Quantitative N_2O desorption during phase IV was tested by analysing the trap outflow during phase V for residual N_2O with an additional single cw-QCLAS analyser in a flow-through mode as described above. At the onset of phase V, small amounts (2 nmol) of residual N_2O were detected, which is < 0.1 % of total adsorbed N_2O. This N_2O might also be caused by micro-leaks, e.g. due to switching of solenoid valves. In addition, quantitative N_2O recovery was assured by an experiment preconcentrating N_2O with distinct ambient and above ambient N_2O mole fractions and yielding corresponding amounts of N_2O (section 3.2.2). One advantage of the TREX-QCLAS technique is that isotope fractionation during N_2O preconcentration can be tested by subsequent dilution and preconcentration of calibration gases (i.e. A and C). In a set of experiments no significant isotopic fractionation for N_2O preconcentration using HayeSep D was detected (< 0.1 ‰) [29].

3.1.2 Temperature stabilisation

Temperature changes of a laser spectrometer affect mole fraction and isotope ratio measurements in a number of different ways: First, differences in lower state energies ($\Delta E''$) of the selected ro-vibrational lines induce varying temperature sensitivity of linestrength and therefore of the analysed isotope ratio, in accordance with Equation (1) [32], in which k is the Boltzmann constant, and T is the absolute temperature. The corresponding temperature sensitivities

are 11.3 ‰ K^{-1}, 19.9 ‰ K^{-1} and 18.2 ‰ K^{-1} for the delta values $\delta^{15}N^{\alpha}$, $\delta^{15}N^{\beta}$ and $\delta^{18}O$-N_2O, respectively.

$$\Delta\delta \approx \frac{\Delta E''}{kT}\frac{\Delta T}{T} \qquad (1)$$

This temperature sensitivity of the N_2O linestrength is taken into consideration by TDL Wintel using gas temperature measurements with a precision of 1 mK based on a 10 kΩ thermistor installed in the absorption cell. This temperature correction might be compromised, however, due to temperature inhomogenities within the cell. Second, variations in laser source temperature may affect isotope ratio measurements by changing the wavelength of the emitted laser light. This effect was tested experimentally, where the laser temperature was changed gradually by 0.01 K during a measurement, which induced a shift in the emission frequency of the laser source and led to significant changes in the analyzed isotope ratios, as demonstrated Figure 5.

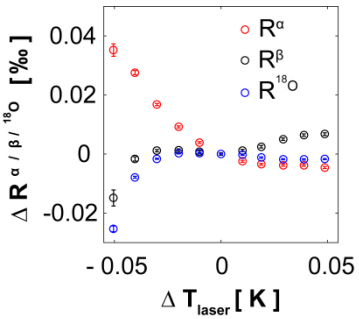

Figure 5 Influence of changes in the laser temperature on isotope ratio measurements. R^{α}, R^{β} and R^{18O} are corresponding to the ratios $^{14}N^{15}N^{16}O$ / $^{14}N^{14}N^{16}O$, $^{15}N^{14}N^{16}O$ / $^{14}N^{14}N^{16}O$ and $^{14}N^{14}N^{18}O$ / $^{14}N^{14}N^{16}O$, respectively. Error bars indicate one standard deviation for measured 1 second values. Under standard operation, deviations of the laser wavelength are precluded by an active control mechanism adjusting the laser temperature accordingly. However, this temperature correction may be compromised, e.g. due to temperature inhomogenities within the cell.

Larger changes in the wavelength of the laser source are precluded by an active feedback control mechanism adjusting the laser temperature.

Third, ambient temperature variations were found to affect the spectrometer operation and performance, mainly by having an influence on the spectrometer optics (precision) and elec-

tronics (drift). A detailed investigation of the various effects is, however, beyond the scope of this paper.

To reduce all of the above effects of temperature variability, the temperature stabilization of the laser spectrometer was greatly improved by embedding the QCLAS into a custom-built thermal insulation box (TB). The TB is made up of aluminium cover plates attached to an aluminium cage. It is temperature-stabilized by four interconnected 4-pass cold plates (Lytron Inc., Woburn, MA, USA) and insulated on the outside with elastomer foam (Armaflex 32 mm, Regisol AG, Switzerland). Coolant circulation and heat discharge is performed by the same thermoelectric recirculating liquid chiller (ThermoRack 401, Solid State Cooling Systems, USA) that is used for temperature stabilization of the spectrometer optics and the laser source. The TB reduced temperature variability by a factor of 40, thus an ambient temperature variation of 2 K h^{-1} resulted in within TB temperature changes of < 0.05 K h^{-1}. In parallel, the laser temperature and the temperature of the sample gas was stabilized in a similar way Figure 6).

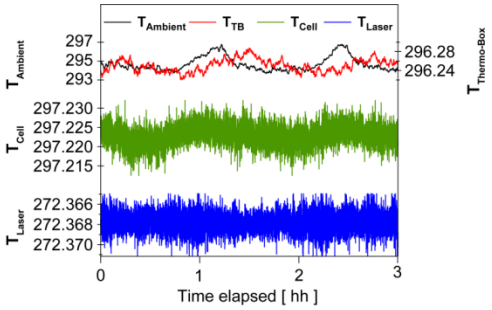

Figure 6 Temperature stability of the spectrometer using a thermal insulation box (TB). Changes in ambient temperature ($T_{Ambient}$) are reduced by a factor 40 (T_{TB}). While the gas temperature in the absorption cell (T_{Cell}) still exhibits systematic changes concurrent with ambient temperature, no effects are apparent for the laser temperature (T_{Laser}). All values are given in Kelvin [K].

3.2 Performance characteristics

3.2.1 QCLAS precision and drift

Precision and drift of the QCLAS were characterised using the Allan variance technique [37]. Measurements were conducted using calibration gas (90 ppm N_2O) at a cell pressure of 20 hPa with 1 Hz temporal resolution (Figure 7).

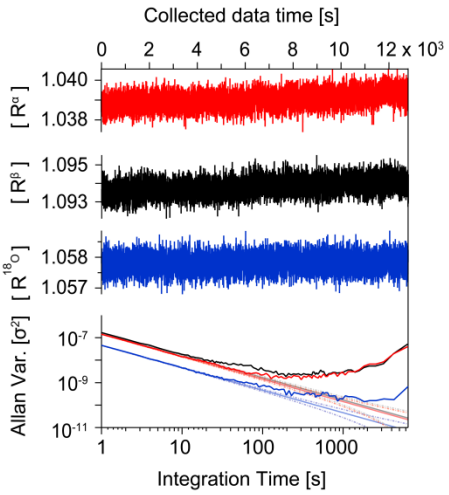

Figure 7 Allan variance plot for N_2O isotpolocule ratios R^{α}, R^{β} and R^{18O}, corresponding to $^{14}N^{15}N^{16}O$ / $^{14}N^{14}N^{16}O$, $^{15}N^{14}N^{16}O$ / $^{14}N^{14}N^{16}O$ and $^{14}N^{14}N^{18}O$ / $^{14}N^{14}N^{16}O$, respectively.

Based on Figure 7, an optimum integration time of around 1000 s was derived, corresponding to a root mean square of the Allan variance minimum of < 0.05 ‰ for isotopic ratio measurements of R^{α}, R^{β} and R^{18O}, corresponding to $^{14}N^{15}N^{16}O$ / $^{14}N^{14}N^{16}O$, $^{15}N^{14}N^{16}O$ / $^{14}N^{14}N^{16}O$ and $^{14}N^{14}N^{18}O$ / $^{14}N^{14}N^{16}O$, respectively (Table 2).

Table 2 Allan precision (σ) of the presented single cw-QCLAS for isotopocule ratios. R^{α}, R^{β} and R^{18O} refer to the ratios $^{14}N^{15}N^{16}O$ / $^{14}N^{14}N^{16}O$, $^{15}N^{14}N^{16}O$ / $^{14}N^{14}N^{16}O$ and $^{14}N^{14}N^{18}O$ / $^{14}N^{14}N^{16}O$, respectively. t_{int} is the optimal integration time in seconds.

Ratio	t_{int} [s]	σ [‰]
R^{α}	512	0.044
R^{β}	610	0.049
R^{18O}	1829	0.012

3.2.2 Mole Fraction Measurements

Pressurized air samples with distinct ambient and above ambient N_2O mole fractions of 326 ± 0.03, 339.2 ± 0.06 and 375.9 ± 0.26 ppb N_2O, were repeatedly analysed using the newly de-

veloped TREX-QCLAS technique. N_2O mole fractions were linked to the NOAA ESRL WMO-N2O-X2006A calibration scale by previous analysis at the World Calibration Centre Empa (WCC) using a single cw-QCLAS (2199.7 cm^{-1}, CW-QC-TILDAS-76-CS; Aerodyne Research Inc., Billerica, USA). Repeated (n = 5) measurements with TREX-QCLAS resulted in standard deviations of 1.0 ppb, 0.43 ppb and 0.53 ppb for the three gases, respectively (Figure 8). The repeatability is thus slightly inferior compared to results by Wolf et al. [24], but superior to recently developed coupled preconcentration IRMS [16] (approx. 1.5 ppb). To achieve the more demanding WMO compatibility goal of 0.1 ppb, additional measurements by CRDS or QCLAS are required [36, 38]. N_2O mole fractions analysed by TREX-QCLAS agreed with mole fractions assigned by the World Calibration Center (WCC). This confirms both quantitative recovery of N_2O after preconcentration and the linearity of the TREX-QCLAS technique.

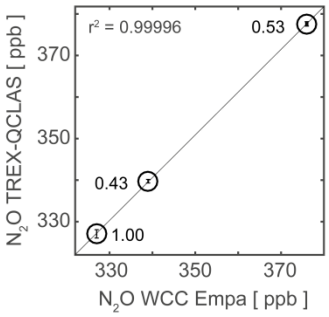

Figure 8 N_2O mole fractions of three cylinders of pressurized ambient air analysed by TREX-QCLAS and plotted versus N_2O mole fractions on the NOAA ESRL WMO-N2O-X2006A calibration scale (WCC-Empa). The numbers given next to the measurement points refer to the standard deviation of repeated measurements (n=5). The r^2 value denotes the correlation between TREX-QCLAS and WCC Empa measurements.

3.2.3 Repeatability of TREX-QCLAS and compatibility to IRMS

The repeatability of the TREX-QCLAS system was assessed through repeated measurements of compressed ambient air. As shown in Figure 9, the standard deviations of repeated measurements were 0.09, 0.13 and 0.17 ‰ for $\delta^{15}N^{\alpha}$, $\delta^{15}N^{\beta}$ and $\delta^{18}O$, respectively. The achieved repeatability is thus comparable to benchmark values achieved in our own laboratory and by other laboratories using more bulky and thus less flexible analytical instrumentation [16, 24, 25].

Table 3 Comparison of the analytical repeatability for N_2O delta values achieved within this study in comparison to benchmark literature data.

	Repeatability (1 standard deviation) [‰]		
Instrument	$\delta^{15}N^{\alpha}$	$\delta^{15}N^{\beta}$	$\delta^{18}O$
TREX-QCLAS (this work)	0.09	0.13	0.17
Wolf et al. $QCLAS_1$ [24]	0.20	0.12	0.11
Harris et al. $QCLAS_2$ [25]	0.08	0.11	0.10
Toyoda et al. IRMS [16]	0.19	0.30	0.23

In parallel, the N_2O isotopic composition of the pressurized air cylinder was analysed by IRMS at Tokyo Institute of Technology (TIT). Results from both laboratories agreed within the expanded standard uncertainty for repeated measurements (Table 3 and Figure 9).

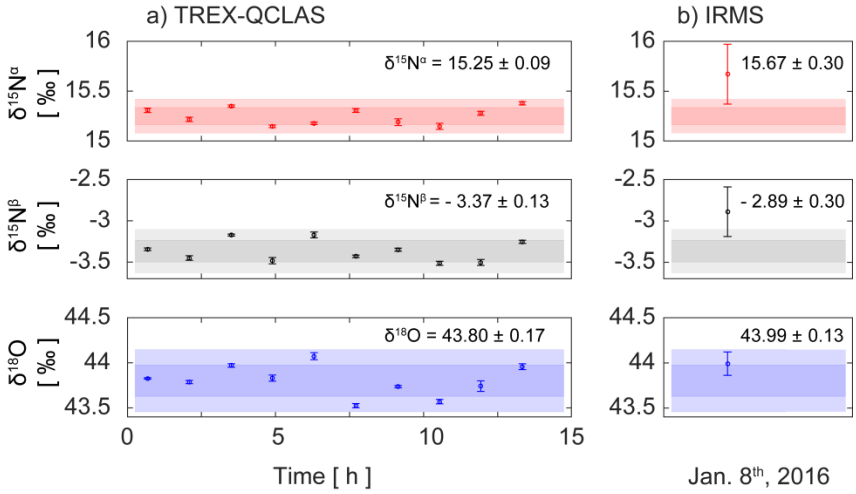

Figure 9 a) Repeated measurements of pressurized ambient air with the TREX-QCLAS technique (error bars refer to one standard deviation [1σ]) and b) isotope-ratio mass-spectrometry at Tokyo Institute of Technology (error bars refer to 1σ for repeated measurements). Dark shades refer to 1σ for repeated TREX-QCLAS measurements, whereas light shaded areas refer to 2σ. Results of both techniques agree within their expanded uncertainty.

4 Conclusions

In this study, a fully-automated and compact TREX-QCLAS instrument was developed for simultaneous measurement of the four N_2O isotopic species $^{14}N^{14}N^{16}N$, $^{14}N^{15}N^{16}O$, $^{15}N^{14}N^{16}O$ and $^{14}N^{14}N^{18}O$. The system demonstrates a repeatability of 0.09, 0.13 and 0.17 ‰ for measuring $\delta^{15}N^{\alpha}$-N_2O, $\delta^{15}N^{\beta}$-N_2O and $\delta^{18}O$-N_2O, respectively. The repeatability is thus sufficient to resolve and interpret biogeochemical as well as industrial emission processes in near-source

studies and isotopic changes in ambient N_2O at remote locations. The presented instrumentation enables real-time analysis of N_2O isotopologues with a temporal resolution of < 1 hr^{-1} which is sufficient for applications in atmospheric monitoring. Furthermore, thanks to a relatively large HayeSep D trap, the system has potential for measurements of clumped N_2O isotopes or other very rare trace gases. In summary, the TREX-QCLAS technique provides a convenient solution for real-time high-precision ambient N_2O isotopic composition measurements, which further improve our understanding of N_2O cycles and give a basis for developing N_2O mitigation strategies.

5 Acknowledgements

We would like to acknowledge the Swiss National Science Foundation for financially supporting this project under Grant No. 200021L_150237. Sakae Toyoda, Naohiro Yoshida and Yuma Watanabe are kindly acknowledged for conducting IRMS measurements within the inter-laboratory comparison conducted in early 2016. Furthermore, we would like to thank Marco Weber for his technical support during the construction of the TREX device and Juanfernando Angel-Ramelli for his support with LabVIEW adaptations.

6 References

[1] Myhre G, Shindell D, Bréon F-M, Collins W, Fuglestvedt J, Huang J, Koch D, Lamarque J-F, Lee D, Mendoza B, Nakajima T, Robock A, Stephens G, Takemura T, Zhang H. Anthropogenic and Natural Radiative Forcing. In: Stocker TF, Qin D, Plattner G-K, Tignor M, Allen SK, Boschung J, Nauels A, Xia Y, Bex V, Midgley PM, editors. Climate Change 2013: The Physical Science Basis. Contribution of Working Group I to the Fifth Assessment Report of the Intergovernmental Panel on Climate Change. Cambridge, United Kingdom and New York, NY, USA: Cambridge University Press; 2013. 659–740.

[2] Ravishankara AR, Daniel JS, Portmann RW. Nitrous Oxide (N_2O): The Dominant Ozone-Depleting Substance Emitted in the 21st Century. Science. 2009;326:123-125.

[3] Prinn RG, R.F. Weiss, P.B. Krummel, S. O'Doherty, P.J. Fraser, J. Muhle, S. Reimann, M.K. Vollmer, P.G. Simmonds, M. Maione, J. Arduini, C.R. Lunder, N. Schmidbauer, D. Young, H.J. Wang, J. Huang, M. Rigby, C.M. Harth, P.K. Salameh, T.G Spain, L.P. Steele, T. Arnold, J. Kim, O. Hermansen, N. Derek, B. Mitrevski, and R. Langenfelds. The ALE / GAGE AGAGE Network, Carbon Dioxide Information Analysis Center (CDIAC), Oak Ridge National Laboratory (ORNL), U.S. Department of Energy (DOE). 2016.

[4] WMO, GAW. Greenhouse Gas Bulletin, The State of Greenhouse Gases in the Atmosphere Based on Global Observations through 2015. 2016.

[5] Nishina K, Akiyama H, Nishimura S, Sudo S, Yagi K. Evaluation of uncertainties in N_2O and NO fluxes from agricultural soil using a hierarchical Bayesian model. Journal of Geophysical Research-Biogeosciences. 2012;117.

[6] Cavigelli MA, Del Grosso SJ, Liebig MA, Snyder CS, Fixen PE, Venterea RT, Leytem AB, McLain JE, Watts DB. US agricultural nitrous oxide emissions: context, status, and trends. Front Ecol Environ. 2012;10:537-546.

[7] Herrero M, Henderson B, Havlik P, Thornton PK, Conant RT, Smith P, Wirsenius S, Hristov AN, Gerber P, Gill M, Butterbach-Bahl K, Valin H, Garnett T, Stehfest E. Greenhouse gas mitigation potentials in the livestock sector. Nature Clim. Change. 2016;6:452-461.

[8] Decock C, Six J. On the potential of $\delta^{18}O$ and $\delta^{15}N$ to assess N_2O reduction to N_2 in soil. Eur J Soil Sci. 2013;64:610-620.

[9] Yoshida N, Toyoda S. Constraining the atmospheric N_2O budget from intramolecular site preference in N_2O isotopomers. Nature. 2000;405:330-334.

[10] Toyoda S, Yoshida N. Determination of Nitrogen Isotopomers of Nitrous Oxide on a Modified Isotope Ratio Mass Spectrometer. Anal Chem. 1999;71:4711-4718.

[11] Brenninkmeijer CAM, Röckmann T. Mass spectrometry of the intramolecular nitrogen isotope distribution of environmental nitrous oxide using fragment-ion analysis. Rapid Commun Mass Spectrom. 1999;13:2028-2033.

[12] Werner RA, Brand WA. Referencing strategies and techniques in stable isotope ratio analysis. Rapid Commun Mass Spectrom. 2001;15:501-519.

[13] Mohn J, Gutjahr W, Toyoda S, Harris E, Ibraim E, Geilmann H, Schleppi P, Kuhn T, Lehmann MF, Decock C, Werner RA, Yoshida N, Brand WA. Reassessment of the

NH_4NO_3 thermal decomposition technique for calibration of the N_2O isotopic composition. Rapid Commun Mass Spectrom. 2016;30:2487-2496.

[14] Sutka RL, Ostrom NE, Ostrom PH, Breznak JA, Gandhi H, Pitt AJ, Li F. Distinguishing nitrous oxide production from nitrification and denitrification on the basis of isotopomer abundances. Appl Environ Microbiol. 2006;72:638-644.

[15] Decock C, Six J. How reliable is the intramolecular distribution of N-15 in N_2O to source partition N_2O emitted from soil? Soil Biol Biochem. 2013;65:114-127.

[16] Toyoda S, Yoshida N. Development of automated preparation system for isotopocule analysis of N_2O in various air samples. Atmos Meas Tech. 2016;9:2093-2101.

[17] Waechter H, Mohn J, Tuzson B, Emmenegger L, Sigrist MW. Determination of N_2O isotopomers with quantum cascade laser based absorption spectroscopy. Opt Express. 2008;16:9239-9244.

[18] Erler DV, Duncan TM, Murray R, Maher DT, Santos IR, Gatland JR, Mangion P, Eyre BD. Applying cavity ring-down spectroscopy for the measurement of dissolved nitrous oxide concentrations and bulk nitrogen isotopic composition in aquatic systems: Correcting for interferences and field application. Limnol Oceanogr Methods. 2015;13:391-401.

[19] Tuzson B, Henne S, Brunner D, Steinbacher M, Mohn J, Buchmann B, Emmenegger L. Continuous isotopic composition measurements of tropospheric CO_2 at Jungfraujoch (3580 m a.s.l.), Switzerland: real-time observation of regional pollution events. Atmos Chem Phys. 2011;11:1685-1696.

[20] Eyer S, Tuzson B, Popa ME, van der Veen C, Rockmann T, Rothe M, Brand WA, Fisher R, Lowry D, Nisbet EG, Brennwald MS, Harris E, Zellweger C, Emmenegger L, Fischer H, Mohn J. Real-time analysis of delta C-13- and delta D-CH_4 in ambient air with laser spectroscopy: method development and first intercomparison results. Atmos Meas Tech. 2016;9:263-280.

[21] Röckmann T, Eyer S, van der Veen C, Popa ME, Tuzson B, Monteil G, Houweling S, Harris E, Brunner D, Fischer H, Zazzeri G, Lowry D, Nisbet EG, Brand WA, Necki JM, Emmenegger L, Mohn J. In situ observations of the isotopic composition of methane at the Cabauw tall tower site. Atmos Chem Phys. 2016;16:10469-10487.

[22] Yamamoto A, Uchida Y, Akiyama H, Nakajima Y. Continuous and unattended measurements of the site preference of nitrous oxide emitted from an agricultural soil using quantum cascade laser spectrometry with intercomparison with isotope ratio mass spectrometry. Rapid Commun Mass Spectrom. 2014;28:1444-1452.

[23] Mohn J, Steinlin C, Merbold L, Emmenegger L, Hagedorn F. N_2O emissions and source processes in snow-covered soils in the Swiss Alps. Isotopes Environ Health Stud. 2013;49:520-531.

[24] Wolf B, Merbold L, Decock C, Tuzson B, Harris E, Six J, Emmenegger L, Mohn J. First on-line isotopic characterization of N_2O above intensively managed grassland. Biogeosciences. 2015;12:2517-2531.

[25] Harris E, Henne S, Hüglin C, Zellweger C, Tuzson B, Ibraim E, Emmenegger L, Mohn J. Tracking nitrous oxide emission processes at a suburban site with semicontinuous, in situ measurements of isotopic composition. Journal of Geophysical Research: Atmospheres. 2017;122:1850-1870.

[26] Keeling CD. The Concentration and Isotopic Abundances of Carbon Dioxide in Rural and Marine Air. Geochim Cosmochim Acta. 1961;24:277-298.

[27] Miller JB, Tans PP. Calculating isotopic fractionation from atmospheric measurements at various scales. Tellus (B Chem Phys Meteorol). 2003;55:207-214.

[28] Harris E, Nelson DD, Olszewski W, Zahniser M, Potter KE, McManus BJ, Whitehill A, Prinn RG, Ono S. Development of a Spectroscopic Technique for Continuous Online Monitoring of Oxygen and Site-Specific Nitrogen Isotopic Composition of Atmospheric Nitrous Oxide. Anal Chem. 2014;86:1726-1734.

[29] Mohn J, Guggenheim C, Tuzson B, Vollmer MK, Toyoda S, Yoshida N, Emmenegger L. A liquid nitrogen-free preconcentration unit for measurements of ambient N_2O isotopomers by QCLAS. Atmos Meas Tech. 2010;3:609-618.

[30] Mohn J, Tuzson B, Manninen A, Yoshida N, Toyoda S, Brand WA, Emmenegger L. Site selective real-time measurements of atmospheric N_2O isotopomers by laser spectroscopy. Atmos Meas Tech. 2012;5:1601-1609.

[31] Schupp M, Bergamaschi P, Harris GW, Crutzen PJ. Development of a tunable diode laser absorption spectrometer for measurements of the 13C12C ratio in methane. Chemosphere. 1993;26:13-22.

[32] Bergamaschi P, Schupp M, Harris GW. High-Precision Direct Measurements of (Ch4)-C-13/(Ch4)-C-12 and (Ch3d)-C-12/(Ch4)-C-12 Ratios in Atmospheric Methane Sources by Means of a Long-Path Tunable Diode-Laser Absorption Spectrometer. Appl Opt. 1994;33:7704-7716.

[33] Aellen T, Blaser S, Beck M, Hofstetter D, Faist J, Gini E. Continuous-wave distributed-feedback quantum-cascade lasers on a Peltier cooler. Appl Phys Lett. 2003;83:1929-1931.

[34] Curl RF, Capasso F, Gmachl C, Kosterev AA, McManus B, Lewicki R, Pusharsky M, Wysocki G, Tittel FK. Quantum cascade lasers in chemical physics. Chem Phys Lett. 2010;487:1-18.

[35] McManus JB, Kebabian PL, Zahniser MS. Astigmatic mirror multipass absorption cells for long-path-length spectroscopy. Appl Opt. 1995;34:3336-3348.

[36] Aerodyne Research Inc., Nitrous Oxide Monitors. Billerica, MA, USA. 2016 [cited 2016 December 22]. Available from: http://www.aerodyne.com/products/nitrous-oxide-monitors.

[37] Werle P, Mucke R, Slemr F. The Limits of Signal Averaging in Atmospheric Trace-Gas Monitoring by Tunable Diode-Laser Absorption-Spectroscopy (Tdlas). Appl Phys B. 1993;57:131-139.

[38] Picarro, Inc., Atmospheric N_2O / CO Mid-IR CRDS Analyzer. Santa Clara, CA, USA. 2016 [cited 2016 December 22]. Available from: http://www.picarro.com/products_solutions/trace_gas_analyzers/n2o_co_h2o.

[39] Rothman LS, Rinsland CP, Goldman A, Massie ST, Edwards DP, Flaud JM, Perrin A, Camy-Peyret C, Dana V, Mandin JY, Schroeder J, McCann A, Gamache RR, Wattson RB, Yoshino K, Chance KV, Jucks KW, Brown LR, Nemtchinov V, Varanasi P. The HITRAN molecular spectroscopic database and HAWKS (HITRAN Atmospheric Workstation): 1996 edition. J Quant Spectros Radiat Transfer. 1998;60:665-710.